ELSEVIER

Polymer 42 (2001) 2101–2112

polymer

www.elsevier.nl/locate/polymer

An investigation into the relationship between processing, structure and properties for high-modulus PBO fibres. Part 1. Raman band shifts and broadening in tension and compression

T. Kitagawa[a], K. Yabuki[a], R.J. Young[b,*]

[a]*Toyobo Research Center Co. Ltd., Research Centre, Ohtsu City, Shiga 520-0292, Japan*
[b]*Materials Science Centre, University of Manchester and UMIST, Manchester M1 7HS, UK*

Received 20 December 1999; received in revised form 12 May 2000; accepted 26 July 2000

Abstract

This study is concerned with an investigation into the relationship between morphology and mechanical properties for poly(*p*-phenylene benzobisoxazole) (PBO) fibres performed using Raman spectroscopy. The three fibres studied have different modulus values (in the range 180–360 GPa), as a result of different processing conditions leading to different molecular orientation and the presence of density fluctuations along the fibre axis. It is found that the 360 GPa modulus fibre has a strain-induced Raman band shift value of -12 cm^{-1}/% which is the highest reported value for aromatic polymer fibres such as PBO and *p*-aramids. The strain-induced Raman band broadening value of this fibre is the lowest among the fibres studied. Compressive strengths for the PBO fibres were also measured and found to be similar (0.29–0.35 GPa). It was also shown that the Raman band broadening becomes less in compression, which is different from the behaviour of carbon fibres and a characteristic feature of PBO fibres. The relationship between the band broadening and fibre morphology is discussed in detail.

Keywords: Raman spectroscopy; PBO fibres; Mechanical properties

1. Introduction

The PBO (poly-*p*-phenylene benzobisoxazole) high-modulus, high-strength super fibre has been commercialised by Toyobo Co. Ltd. under the trade name of Zylon®. It is based upon the molecule:

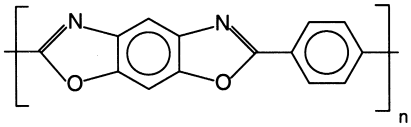

The Young's modulus of PBO is higher than that of any other commercial fibre, but there still exists a gap between the values of actual and theoretical moduli. We have recently succeeded in improving PBO fibres further in laboratory experiments by adopting a non-aqueous coagulation system and a heat-treatment method [1]. It is important to implement a slow coagulation process during fibre production because the pre-structure of the fibre induced before heat-treatment determines both the final fibre structure and its mechanical properties. The modulus of the improved PBO fibre thus obtained can be as high as 360 GPa. The fibres also show an absence of the four-point small-angle X-ray scattering (SAXS) pattern that is characteristic of the morphology of heat-treated PBO fibre obtained using the normal (aqueous) coagulation process [1]. The apparent crystal size measured is almost the same as for the HM fibre and the molecular orientation is slightly higher for the improved fibre. This implies that factors other than just molecular orientation are concerned with improving moduli. It is thus the objective of this study to use Raman spectroscopy, which is a powerful technique to detect molecular deformation in fibres under stress [2–5], to elucidate the mechanism of modulus improvement for this new experimental PBO fibre. This first paper is concerned with the relationship between Raman band peak shift, peak broadening, and fibre morphology for PBO fibres processed under different conditions.

2. Materials and experimental methods

2.1. Materials

The three PBO sample fibres investigated were AS, HM

* Corresponding author.

0032-3861/01/$ - see front matter
PII: S0032-3861(00)00571-1

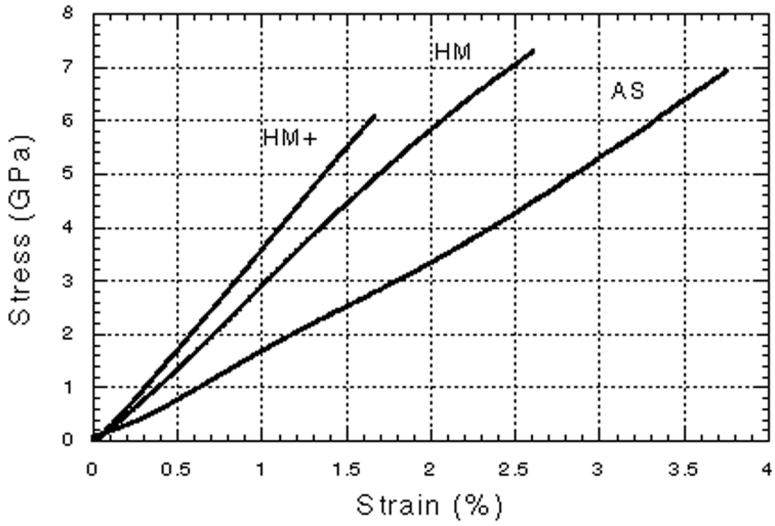

Fig. 1. Stress–strain curves for the three different types of PBO fibre.

(commercial fibers) and HM + (an improved experimental fibre). PBO fibres are spun using the dry-jet wet-spinning method [6]. The AS fibre is coagulated in aqueous phosphoric acid, washed with a fresh water, then dried in a oven and wound up. The exact processing conditions are proprietary but the HM fibre is made by the heat treatment of AS fibres under tension. The HM + fibre is produced in a similar way to HM using a different, non-aqueous coagulation bath, followed by washing, drying, and heat treatment with tension [1].

2.2. Mechanical testing

The fibre modulus and strength were measured using an Instron 1121 universal testing machine. To ensure good adhesion of the fibre during testing, a monofilament was mounted across a cardboard window using quick-setting two-part cold-curing epoxy resin. It was stored at least two days to allow the resin to set completely prior to testing. Gauge lengths of 20, 50 and 100 mm were employed with at least 20 specimens tested at each gauge length using a cross-head speed of 1%/min. All the tests were carried out at 23 ± 2°C and a relative humidity of 50 ± 5%. The load-time data were stored in a digital form using a Macintosh computer and Workbench 3.1 software. The data were converted into stress–strain curves; the stress was determined from the load and fibre cross-sectional area and the strain calculated from the gauge length and cross-head displacement.

Individual fibres were examined on a Philips 505M scanning electron microscope (SEM) operated at 10 kV. The magnification was calibrated using a standard specimen with 2160 lines/mm. The fibre was coated with a thin layer of gold to avoid charge build up during SEM operation and the diameter was obtained from the average of at least 25 measurements.

2.3. Raman spectroscopy

Raman scattering measurements were conducted under both tensile and compressive loading using a Renishaw System 1000 Raman microprobe with a newly developed 25 mW near infrared laser. The 780 nm laser allows spectra to be obtained from fibres such as PBO with less fluorescence than is found with shorter wavelength radiation. The $50\times$ objective lens of an Olympus BH-2 optical microscope is used both to focus the laser beam on the specimen surface (spot size of ~ 2 μm in diameter) and to collect the 180° back-scattered radiation. A highly sensitive Renishaw Charge-Coupled Device (CCD) camera was used to collect the Raman spectra. The degree of peak shift and peak broadening under stress of the 1618 cm^{-1} PBO Raman band, corresponding to the vibration of the backbone *p*-phenylene ring [4], were determined. The digital data were processed on a computer with the Renishaw analysis software in which a Lorentzian curve-fitting procedure was used to determine the peak position and width.

In order to apply simultaneously tensile strain to a single fibre and obtain a Raman spectrum, monofilaments of 50 mm gauge length were fixed using cyanoacrylate adhesive between aluminium foil tabs. One end of the tab was connected to a miniature load cell to measure load and the other to a micrometer to apply and monitor the fibre displacement, with a precision of ± 0.005 mm. For compressive deformation, a four-point bending method was adopted [3]. An individual single fibre was placed on the surface a poly(methyl methacrylate (PMMA) plate and covered with a thin layer of PMMA/chloroform solution that was allowed to dry. The strain was monitored using a resistance strain gauge (Measurements Group, Inc.) carefully fixed next to the fibre on the plate using cyanoacrylate adhesive.

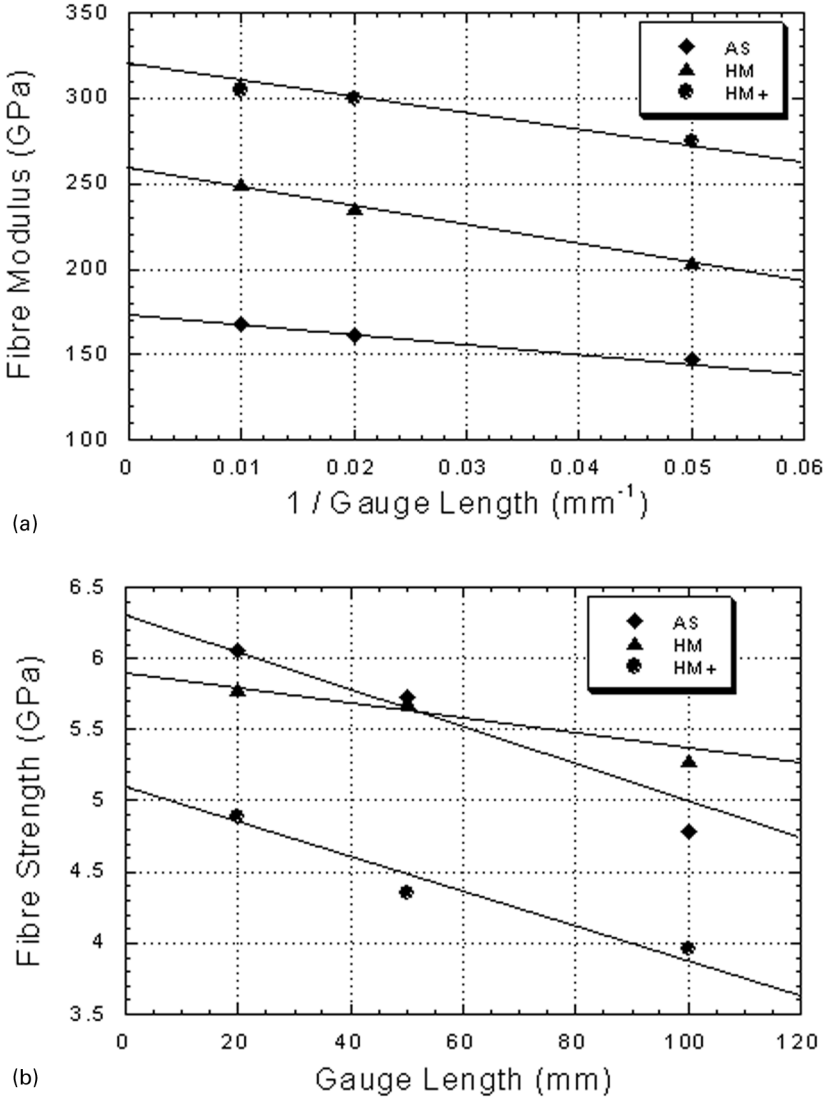

Fig. 2. (a) Dependence of PBO fibre modulus upon the reciprocal of the gauge length. (b) Dependence of the PBO fibre strength upon the gauge length.

3. Results and discussion

3.1. Mechanical testing

Typical stress–strain curves are shown in Fig. 1 for the three PBO fibres. It appears that there is some strain hardening for all three fibres. The strain–stress curve of AS fibre increases in slope until ~0.7% strain, the slope then become lower at intermediate strain, and finally increases again in the high-stress region. The stress–strain curve for the HM fibre decreases in slope after the stress–strain curve reaches its steepest point around 1.0% strain. For the HM + fibre, which has the highest modulus value of the three fibres, the curve increases in slope from 0 to 1.2% strain, after which the slope becomes less. This shape is clearly different from that of the HM fibre and interesting because even the

Table 1
Mechanical properties of the PBO fibres ((±): standard deviation; method 1: single filament tensile test; method 2: bundle yarn (JIS 1013))

Fibre	Diameter (μm)	Method 1		Method 2	
		Strength (GPa)	Modulus (GPa)	Strength (GPa)	Modulus (GPa)
AS	11.9	6.30 (± 0.88)	173 (± 16.3)	5.55	187
HM	12.0	5.90 (± 0.79)	260 (± 24.4)	5.59	258
HM +	12.2	5.10 (± 0.76)	320 (± 29.7)	4.72	352

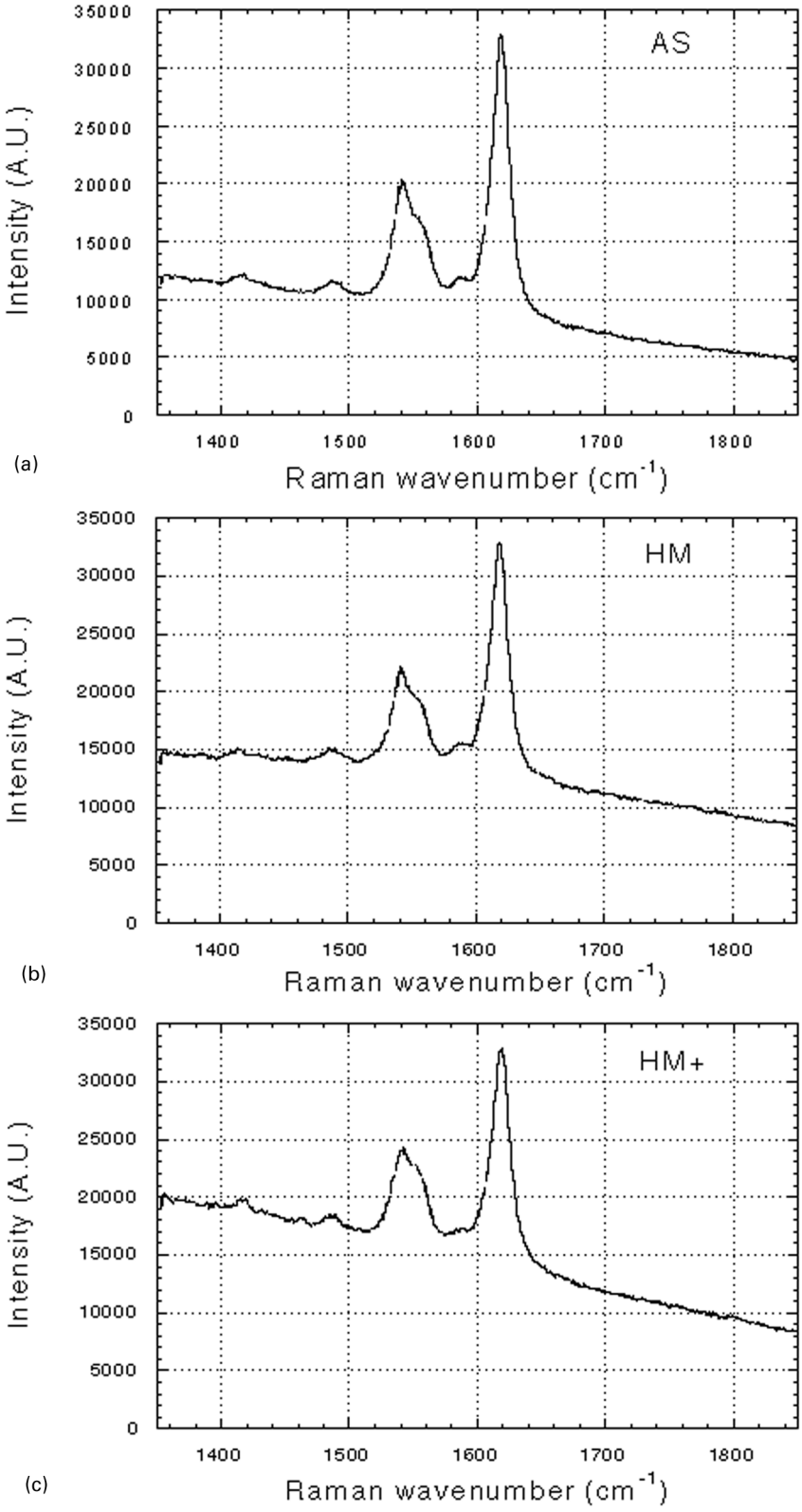

Fig. 3. Raman spectra for the three different PBO fibres.

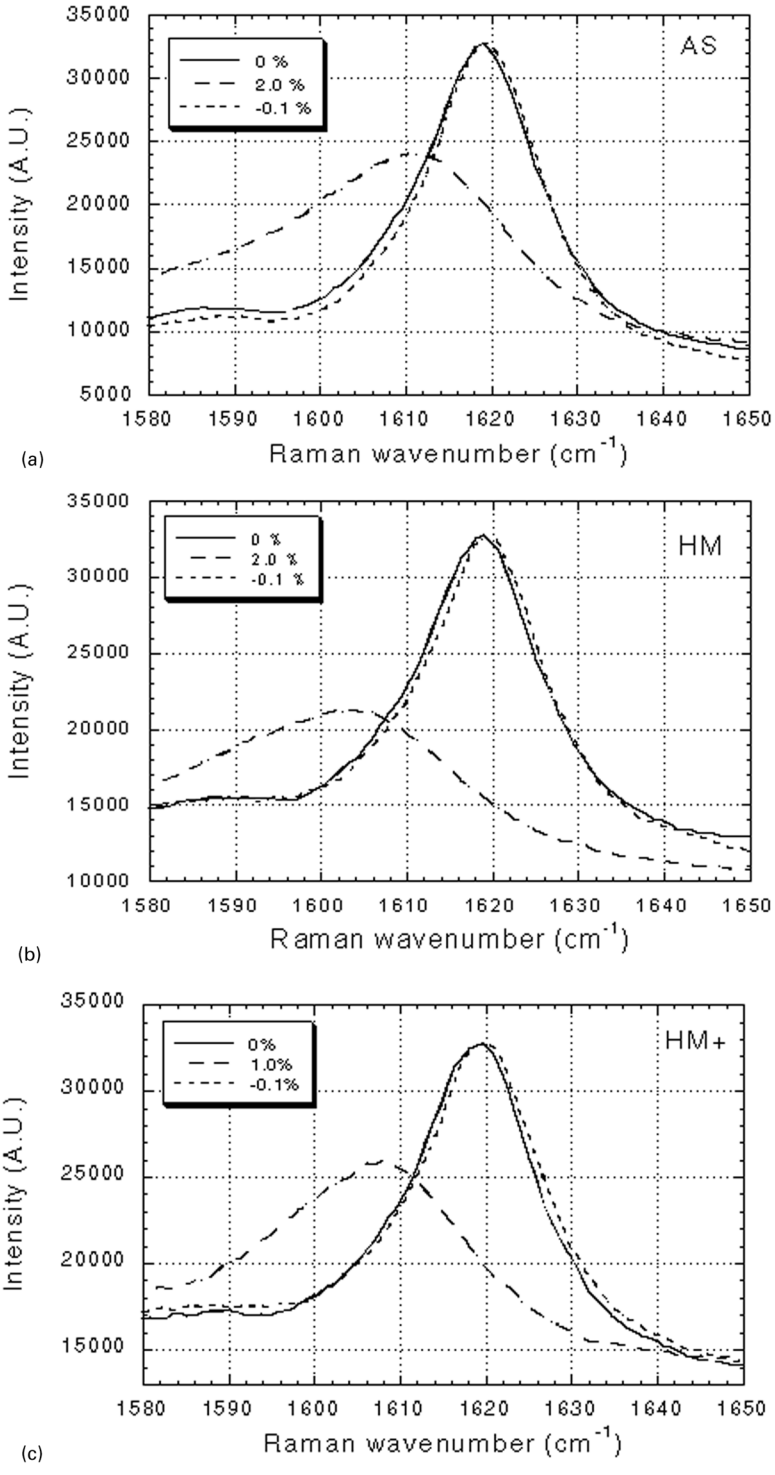

Fig. 4. Deformation-induced Raman band shifts for the three different PBO fibres.

heat-treated HM + fibre seems to show some limited strain hardening. It is also noteworthy that the stress–strain curve for the AS fibre includes an intermediate region in which strain dependence of Young's modulus decreases before the hardening starts. Both of these phenomena cannot be explained solely by an improvement in molecular orientation [4] and must be therefore be related to existence of density fluctuations along the fibre axis [1].

To estimate the modulus in the absence of end effects and intrinsic fibre strength, the mechanical properties of the fibres were measured using three different gauge lengths. The modulus was determined by extrapolating to infinite

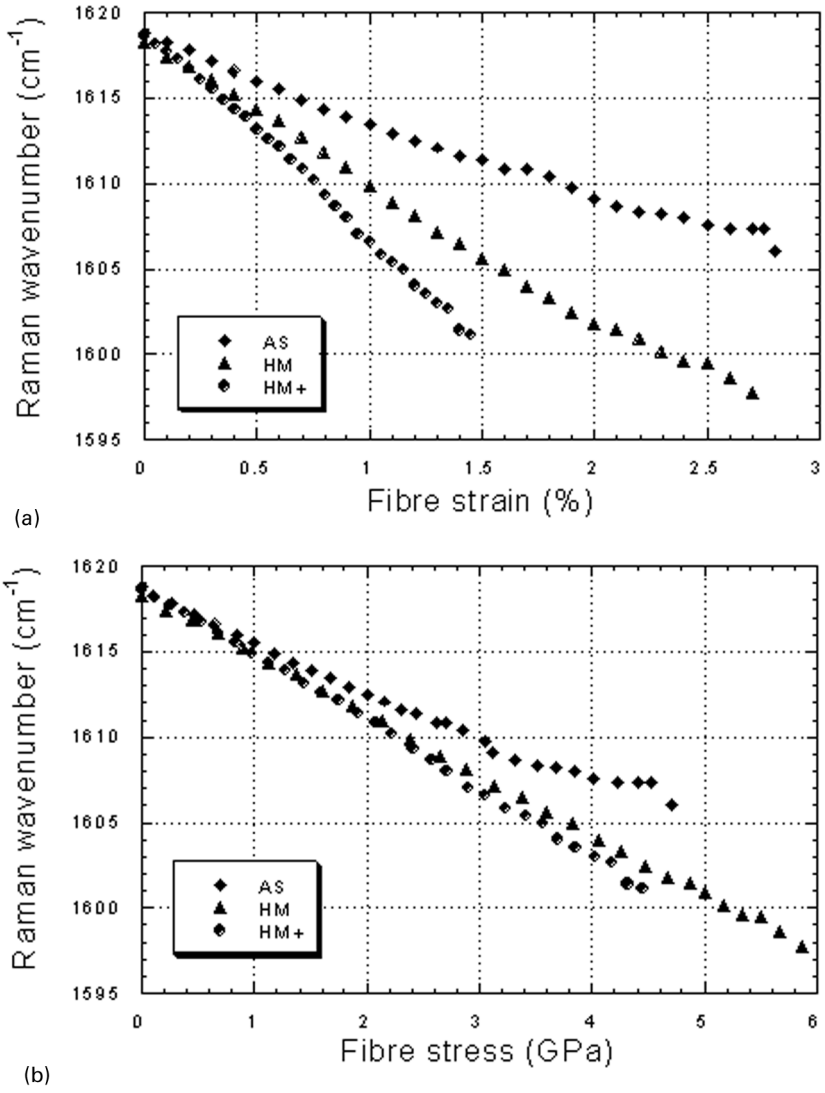

Fig. 5. Dependence of the peak position of the 1618 cm^{-1} Raman band for the three different PBO fibres upon (a) strain and (b) stress.

gauge length as shown in Fig. 2a and the strength by extrapolating to zero gauge length as shown in Fig. 2b. It can be seen that the modulus increases in the order AS < HM < HM + (c.f. Fig. 1) and that the HM + fibre has a slightly lower strength than AS and HM fibres. The mechanical properties of the fibres are summarised in Table 1.

3.2. Raman band peak shifts

Raman spectra measured at zero strain for the three fibres with no background subtraction are shown in Fig. 3. It can be seen that there is an increase in background fluorescence scattering in the order of AS < HM < HM + , but even so the spectra all show well-defined peaks which are far better-defined than those reported previously using a He–Ne laser (632.8 nm) [4]. It is thought that this is due to change of laser wavelength to an IR laser (780 nm) that leads to much lower levels of fluorescence with PBO fibres.

Fig. 4 shows the effect of deformation upon the 1618 cm^{-1} band for the three different types of PBO fibre subject to tensile and compressive strains. The band can be seen to moves towards low wavenumber and broaden with tensile deformation but shift in the opposite direction and then become narrower in compression. This indicates that molecules in the fibres respond to the external deformation and that there is a modification of the strain distribution between the molecules in the fibre. The detailed behaviour of the peak position and shape were analysed in detail using a Lorentzian curve-fitting procedure.

Typical strain-induced Raman band peak shifts for the three PBO fibres are shown in Fig. 5a. It can be seen that the intercepts at zero strain of all the plots have the same value (1618.5 cm^{-1}). The data points for the AS fibre follow a linear line in the low-strain region but deviate at intermediate strain. For the HM and HM + fibres the points lie approximately on straight lines. The strain- and

Table 2
Values of rates of deformation-induced Raman band shifts and broadening ((±): standard deviation)

Fibre	Strain-induced		Stress-induced	
	Raman band shift (cm^{-1}/%)	Band broadening (cm^{-1}/%)	Raman band shift (cm^{-1}/GPa)	Band broadening (cm^{-1}/GPa)
AS	−4.85 (± 0.40)	3.08 (± 0.33)	−3.27 (± 0.30)	2.09 (± 0.25)
HM	−8.60 (± 0.26)	4.10 (± 0.34)	−3.75 (± 0.40)	1.71 (± 0.25)
HM +	−11.52 (± 1.37)	3.74 (± 0.53)	−4.06 (± 0.34)	1.30 (± 0.09)

stress-induced Raman band shifts were determined from the initial slopes of the curves. It was found that the slopes increased with increasing fibre modulus and the value for the HM + fibre reached −12 cm^{-1}/%, which is the highest value reported for this band in aromatic polymer fibres such as PBO and PPTA (*p*-aramid) [2] with the structure:

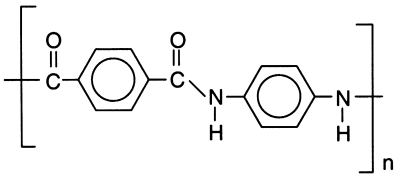

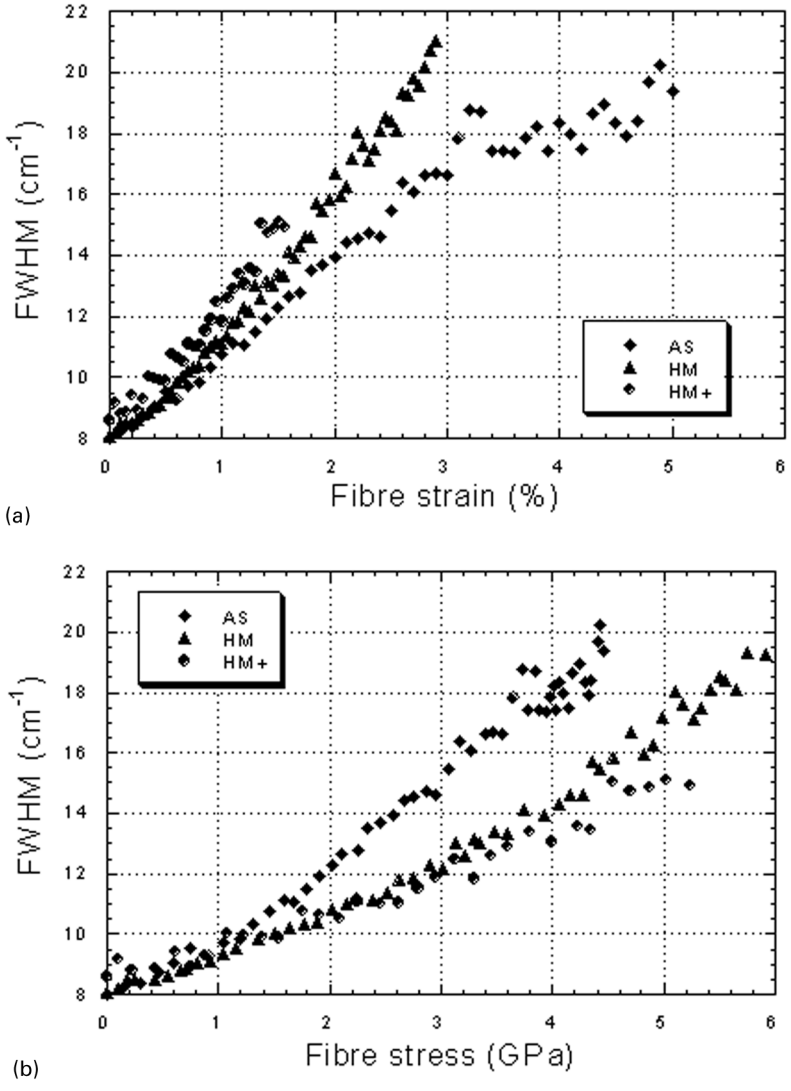

Fig. 6. Dependence of the full width at half maximum height (FWHM) of the 1618 cm^{-1} Raman band for the three different PBO fibres upon (a) strain and (b) stress.

Table 3
Compressive strength data for the PBO fibres determined from Figs. 7–9 ((±), standard deviation)

Fibre	Compressive strength (GPa)
AS	0.29 (± 0.05)
HM	0.36 (± 0.04)
HM +	0.35 (± 0.02)

It is known that the band shift factor in such fibres is controlled by molecular orientation [2,4] and so this very large value must reflect the high-degree of molecular orientation in the HM + fibre.

Deformation-induced Raman band shifts were also determined as a function of stress for the PBO fibres as shown in Fig. 5b. In the literature, the Raman band corresponding to the vibration of the backbone *p*-phenylene ring is reported to have the same stress-induced shift rate (approximately $-4.0\ cm^{-1}$/GPa) for PBO, PPTA, and PET (poly(ethylene terephthalate)) fibres [4,5] i.e. irrespective of materials, when the molecules in the fibre are highly oriented. The molecules in all the PBO fibres are so highly extended that we may assume that they are all strained homogeneously and such that the three fibres should have the same values of stress-induced Raman band shift. Table 2 shows that the values obtained for the HM and HM + fibres follow this rule, but that the AS fibre showed a value significantly lower than $-4\ cm^{-1}$/GPa. It is possible that the assumption of homogeneous strain [4] does not apply exactly and as in the case of some aramid fibres [3] the AS fibre consists of skin-core structure (with inhomogeneity along the radial direction of the fibre cross-section). This leads to a smaller value of band-shift rate due to a low-modulus fibre skin since the Raman spectrum is thought

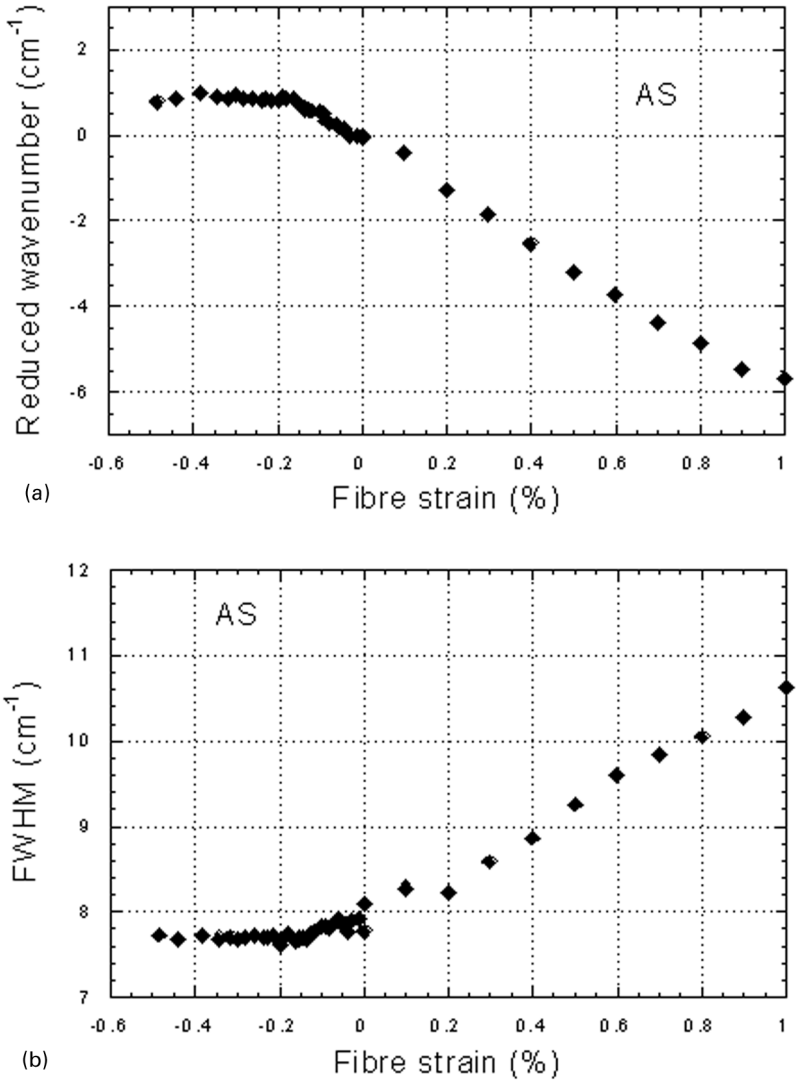

Fig. 7. Behaviour of the 1618 cm^{-1} Raman band for an AS PBO fibre subjected to tensile (positive) and compressive (negative) deformation. (a) Dependence of the peak position upon strain. (b) Dependence of the FWHM upon strain.

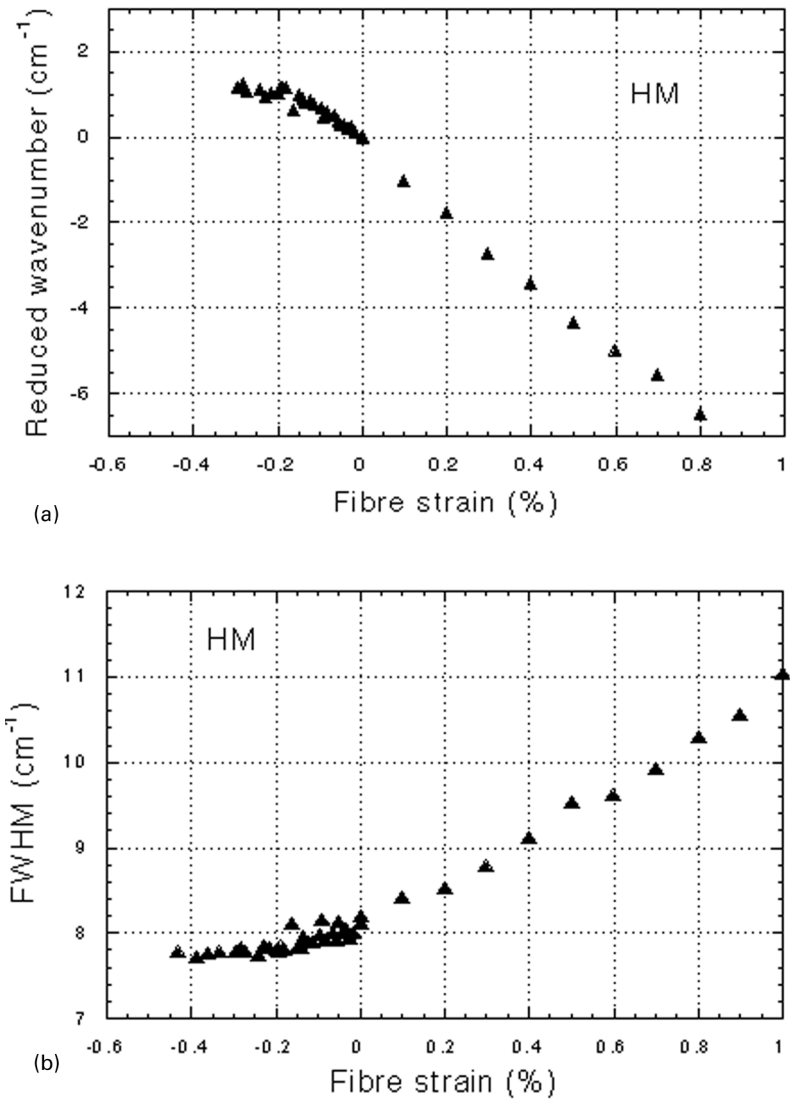

Fig. 8. Behaviour of the 1618 cm^{-1} Raman band for an HM PBO fibre subjected to tensile (positive) and compressive (negative) deformation. (a) Dependence of the peak position upon strain. (b) Dependence of the FWHM upon strain.

to be obtained from the fibre surface region [3]. This phenomenon is presently under investigation using transmission electron microscopy [7,8].

3.3. Raman band broadening

The full width at half maximum (FWHM) values [4] of the Raman bands are plotted against strain and stress in Figs. 6a and b. It can be seen that in each case there is a significant peak broadening that is considered to be due to the stress distribution upon the molecules in the fibres [5]. From the slopes of the plots, the Raman band broadening can be estimated and the values are presented in Table 3. It is seen that the stress-induced Raman band broadening value is the smallest (1.30 cm^{-1}/GPa) among the three fibres for the HM + fibre. The strain-induced Raman band broadening value of HM is less than that of HM + , but larger than that of AS fibre. This difference in band broadening behaviour is thought to be due to the distribution of stress on the molecules in the fibre being increased when the fibres are deformed such that the degree of the increase for HM + fibre is lower than that of the HM fibre. It is also noteworthy that the intercept at zero strain for the HM + fibre (8.6 cm^{-1}) is slightly higher than those of the AS and HM fibres (~8.0 cm^{-1}) which may indicate a higher level of initial residual stress in the HM + fibre.

It is interesting to relate this phenomenon of Raman band broadening to the lack of four-point SAXS pattern [1] for the HM + fibre. This indicates that the HM + fibre has a more homogeneous structure along the fibre axis than the HM fibre. It is possible that the inhomogeneity in the HM fibre comes from the periodicity of ordered and disordered regions; the disordered regions could include molecular chain ends, dislocations, poorer orientation etc. To achieve

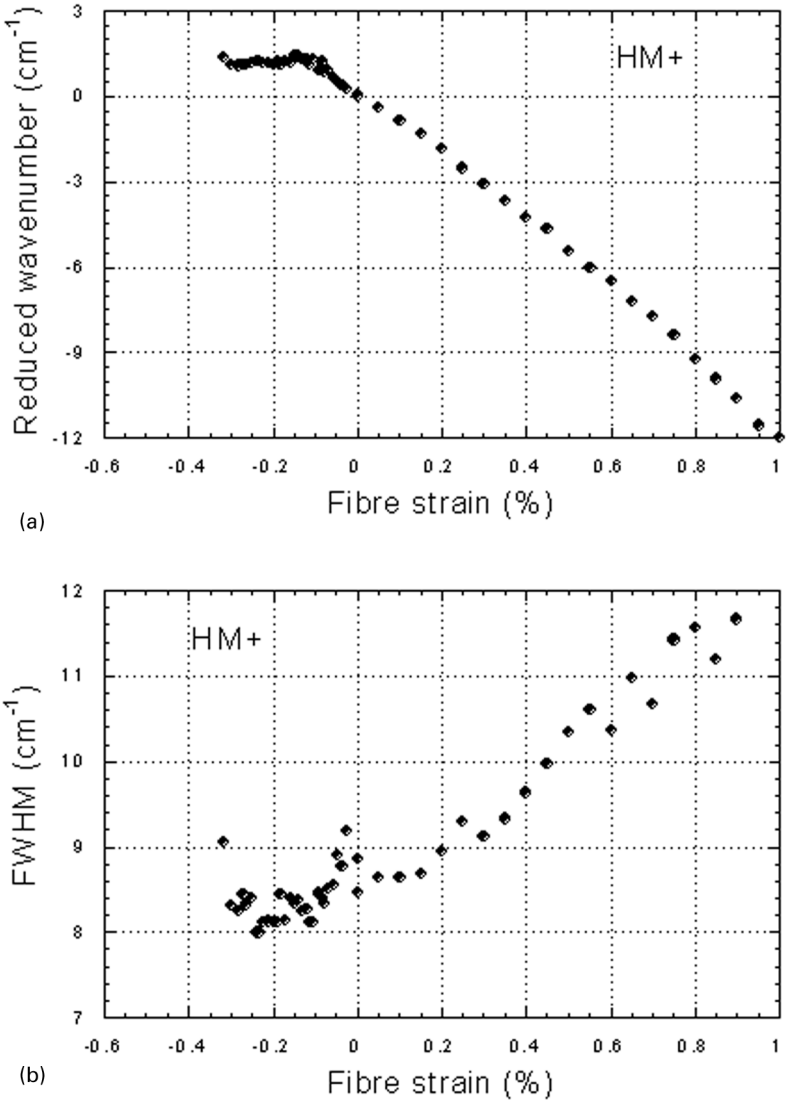

Fig. 9. Behaviour of the 1618 cm^{-1} Raman band for an HM + PBO fibre subjected to tensile (positive) and compressive (negative) deformation. (a) Dependence of the peak position upon strain. (b) Dependence of the FWHM upon strain.

the homogeneous structure, the molecules in HM + fibres must take a more extended form than in the HM fibre. Such a molecular conformation will necessarily cause both the broader FWHM distribution at zero stress and the smaller level of Raman band broadening. In conclusion it is believed that the small value of band broadening for HM + originates from this homogeneous structure. In the final paper of this series [8] this morphological structure will be investigated using high-resolution electron microscopy techniques.

3.4. Compressive deformation

Figs. 7–9 show the variation of the peak positions and FWHM of the 1618 cm^{-1} Raman bands with both tensile and compressive fibre strain for the three types of PBO fibre. It can be seen that there is an approximately linear relation between band position and fibre strain when fibres are deformed in tension. The behaviour in compression, however, is quite different. The band shifts to a higher wavenumber until reaching a maximum value at a critical strain, after which it maintains a plateau value. This behaviour is similar for all the three PBO fibres. At the same time, the FWHM increases in tension but becomes narrower when the fibre is strained in compression until a critical strain value, after which it becomes constant. This critical value of strain is similar the value for which Raman band position reaches a plateau. The compressive strength of the PBO fibres can be estimated from the critical strain required to reach this plateau and the values are tabulated in Table 3. The heat-treated fibres show slightly higher compressive strength values than the AS fibre. These values are significantly less than those obtained for the PIPD fibre "M5" [9] and so it appears that the compressive properties of high-modulus polymer fibres are determined by the basic molecular

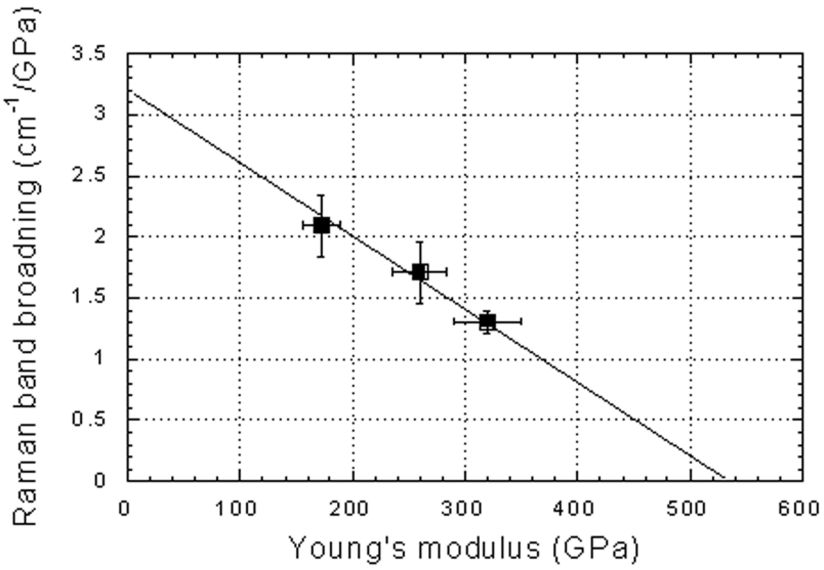

Fig. 10. Dependence of the Raman band broadening upon Young's modulus for the three different PBO fibres.

structure of the fibre; morphological factors have only a secondary effect.

It is interesting to observe that the FWHM narrows in compression, implying that the distribution stress local molecular stress in the fibres is reduced. This behaviour is different from that of other fibres such as carbon fibres [10] that appear to show broadening in both tension and compression. The PBO molecule does not form a three-dimensional crystal structure as in carbon fibres and each molecule is free to adopt different individual conformations. It is possible that residual strain induced in the coagulation and heat-treatment processes is relaxed during compressive deformation leading to the Raman band narrowing.

3.5. Comparison with crystal modulus

The relationship between stress-induced band broadening and fibre modulus is presented in Fig. 10. Measured values of crystal modulus of up to 460–480 GPa have been found for PBO [1,11,12] using X-ray diffraction. Early theoretical calculations of modulus by Wierschke [13] for PBO predicted a modulus value of over 600 GPa whereas a value of 460 GPa has been reported following a theoretical calculation based on lattice mechanics [14]. In Fig. 10 the linear line fit to the data points of the PBO fibres extrapolates to 530 ± 50 GPa for zero band broadening. This value is higher than the measured values of PBO crystal modulus [5,6] but within the range of values calculated theoretically [13,14].

A similar relationship between the Raman band broadening and crystal modulus has also been reported for PPTA aramid fibres [4]. It is thought that Raman peak broadening should occur only in fibres that are not single crystals. This implies that if a fibre showing zero band broadening could be prepared, its measured modulus would equal the crystal modulus. It appears that the peak broadening is controlled by the perfection of the fibre structure; when the fibre is assembled with 100% perfect crystals and there is no disordered region in the fibre (e.g. all the molecules are aligned perfectly to the fibre direction), the peak broadening of the fibre becomes zero and the fibre modulus reaches crystal modulus. Hence, the Raman band broadening is an important parameter that can be used to characterise the relation between the homogeneity of the microstructure of the fibre and its mechanical properties.

3.6. Mechanisms of stress distribution in the fibres

Finally, it is necessary to reconsider the effect of the morphological features of PBO fibres upon their mechanical properties. PBO fibres have only weak inter-molecular linking between neighbouring molecules. Fibres such as PPTA and PIPD [9] with the structure:

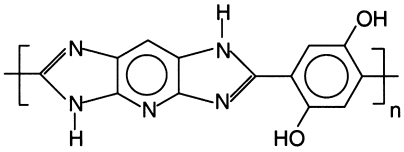

have OH– and NH– groups along the molecule, which lead to intermolecular H-bonding. Wide-angle X-ray diffraction confirms three-dimensional crystallites in PPTA [15] and PIPD [16] but PBO shows translational disorder along the fibre axis in the crystal, which is caused by weak interactions between the molecules [17]. This lack of inter-molecular links will then allow molecular slippage to take place when a PBO fibre is deformed.

It is known that PBO fibres have structural inhomogeneity along the fibre axis. When a fibre is deformed to the axial direction, disordered regions may lead to the onset

of molecular slippage that may propagates to the whole fibre with increasing stress. It is likely that the Raman band broadening observed is the result of such molecular slippage. From this assumption we can also understand why the HM fibre has a high value of the broadening because it has more inhomogeneities than the HM + fibre, as confirmed by an SAXS study [1,17]. It may be possible in future studies to obtain direct evidence of molecular slippage propagating from disordered regions.

4. Conclusions

A newly developed experimental PBO fibre (HM+) with Young's modulus of >320 GPa has been investigated together with commercial AS and HM fibres using Raman spectroscopy. It is found that rate of strain-induced Raman shift for the HM + fibre is the highest among the three fibres, consistent with its high-modulus as a result of its high level of molecular orientation. The values of stress-induced Raman band shift for the PBO fibres are around $-4.0\ cm^{-1}$/GPa except for AS ($-3.3\ cm^{-1}$/GPa). Raman band broadening shift is sensitive to fibre modulus and extinction of an SAXS four-point pattern. There should be a relation between density fluctuation in the fibre structure and the stress distribution of individual molecules that form the fibre structure. In compression the Raman bands narrow. It is believed that in due to the relaxation of residual strain in the fibres induced during processing.

It was not possible to explain why the stress-induced Raman band shift for the AS fibre has a different value from all other aromatic polymer fibres. It is also unclear what is the exact deformation mechanism relating the Raman band broadening to the fibre microstructure. To clarify these matters further, it will be necessary to undertake a transmission electron microscope study to obtain a better understanding of the fibre microstructure [9].

Acknowledgements

The authors are grateful to the EPSRC for financial support in the form of research grants and to Toyobo Co., Ltd for permission to publish the research.

References

[1] Kitagawa T, Ishitobi M, Yabuki K. Journal of Polymer Science: Part B 2000;38:1605.
[2] Young RJ. Journal of the Textile Institute 1995;86:360.
[3] Young RJ, Lu D, Day RJ, Knoff WF, Davis HA. Journal of Materials Science 1992;27:5431.
[4] Yeh W-Y, Young RJ. Polymer 1999;40:857.
[5] Yeh W-Y, Young RJ. Journal of Macromolecular Science: Physics 1998;B37:83.
[6] Yang HH. Aromatic high-strength fibers, SPE Monograph. New York: Wiley, 1989.
[7] Kitagawa T, Yabuki K, Young RJ. Part 2, in preparation.
[8] Kitagawa T, Yabuki K, Wright AC, Young RJ. Part 3, in preparation.
[9] Sirichaisit J, Young RJ. Polymer 1999;40:3421.
[10] Melanitis N, Tetlow PL, Galiotis C, Smith SB. Journal of Materials Science 1994;29:786.
[11] Nishino T, Matsui R, Nakamae Y, Gotoh M, Nagura M. Sen-i Gakkai Preprints 1995;1995:G-149.
[12] Lenhert PG, Adams WW. Materials Research Society Symposium Proceedings 1989;134:329.
[13] Wierschke SG. Materials Research Society Symposium Proceedings 1989;134:313.
[14] Tashiro K, Kobayashi M. Macromolecules 1991;24:3706.
[15] Krause SJ, Vezie DL, Adams WW. Polymer Communications 1989;30:10.
[16] Lammers. PhD thesis. Swiss Federal Institute of Technology, ETH no. 12685, 1998.
[17] Kitagawa T, Murase H, Yabuki K. Journal of Polymer Science: Part B 1998;36:39.